Acta Biomaterialia 18 (2015) 213–225

Contents lists available at ScienceDirect

Acta Biomaterialia

journal homepage: www.elsevier.com/locate/actabiomat

Some design considerations for polymer-free drug-eluting stents: A mathematical approach

Sean McGinty [a,*], Tuoi T.N. Vo [b], Martin Meere [c], Sean McKee [a], Christopher McCormick [d]

[a] Department of Mathematics and Statistics, University of Strathclyde, Glasgow G1 1XH, UK
[b] MACSI, Department of Mathematics and Statistics, University of Limerick, Limerick, Ireland
[c] Department of Applied Mathematics, NUI Galway, Galway, Ireland
[d] Department of Biomedical Engineering, University of Strathclyde, Glasgow G4 0NW, UK

ARTICLE INFO

Article history:
Received 30 September 2014
Received in revised form 15 January 2015
Accepted 10 February 2015
Available online 21 February 2015

Keywords:
Polymer-free stents
Dissolution
Diffusion
Drug release
Nanoporous materials

ABSTRACT

In this paper we provide the first model of drug elution from polymer-free arterial drug-eluting stents. The generalised model is capable of predicting drug release from a number of polymer-free systems including those that exhibit nanoporous, nanotubular and smooth surfaces. We derive analytical solutions which allow us to easily determine the important parameters that control drug release. Drug release profiles are provided, and we offer design recommendations so that the release profile may be tailored to achieve the desired outcome. The models presented here are not specific to drug-eluting stents and may also be applied to other biomedical implants that use nanoporous surfaces to release a drug.

1. Introduction

1.1. Background

Drug-eluting stents (DES) have significantly improved the treatment of coronary heart disease (CHD) and are the current gold standard in percutaneous coronary interventions (PCIs). These small drug-containing mesh-like devices are now routinely inserted into arteries which have become dangerously narrowed due to a condition known as atherosclerosis. Their role is to increase the diameter of the diseased lumen, so that adequate blood flow can be restored. Their predecessor, the so-called bare metal stents, whilst revolutionary at the time, were soon found to be inadequate due to the common occurrence of restenosis (the re-narrowing of the lumen). Subsequent stent designs included an antiproliferative drug designed to prevent smooth muscle cell proliferation and migration which is thought to contribute to restenosis: these are the drug-eluting stents [1]. The drug was typically contained within a polymer coating on the surface of the metal stent. To date there have been several generations of DES, each with design features aimed at improving clinical results. These include multi-layer polymer coatings to help control the release, thinner struts to reduce damage to the arterial tissue and more biocompatible polymer coatings and metal alloys [2]. However, several studies have raised concerns that the permanent presence of a polymer may trigger an allergic reaction and possibly a local vascular inflammatory response in some patients [3,4]. Moreover, several early studies reported evidence of delayed healing of the endothelial cell layer of the arterial wall following DES use, in comparison to bare metal stents [5,6]. These unwanted effects have been associated with the occurrence of late stent thrombosis and sudden cardiac death. With this in mind, cardiologists have recommended that anti-platelet therapy is continued for a full twelve months after stent implantation [1]. Driven by a desire to improve clinical outcomes, newer generation DES have focussed on biodegradable polymers, where the polymer carries and controls the drug release and then completely erodes, and also polymer-free coatings which do not contain any polymer at all. Whilst modelling drug release from stents which contain a non-erodible polymer (e.g. [7–11]) and a biodegradable polymer (e.g. [12–18]) has received much attention in the literature, the modelling of polymer-free DES has not. This is somewhat surprising, especially since a recent drug-eluting stent review [19] reports that "...polymer-free, controlled-release stent designs may become the substrate of choice in the longer-term, especially if they exhibit non-inferiority in terms of restenosis reduction".

To date, several polymer-free stents have been designed and some of them have reached the market. There have, however, been

* Corresponding author. Tel.: +44 141 5483286.
E-mail address: s.mcginty@strath.ac.uk (S. McGinty).

http://dx.doi.org/10.1016/j.actbio.2015.02.006
1742-7061/

many challenges for the stent manufacturers. For example, they have had to address how the drug release can be controlled with no polymer, how the drug can be adequately adhered to the stent surface and have had to consider carefully the stent platform material to ensure that it is biocompatible. The stent manufacturers have adopted different approaches in designing these stents, which can be roughly separated into four categories [20]: macroporous, microporous, nanoporous and smooth surface. Macroporous DES utilise precise manufacturing processes to accurately inlay the drug into holes or slits in the body of the stent. Some examples include the Janus Flex (Sorin Group), Conor Stent (Conor Medsystems), CoStar (Conor Medsystems), and Nevo (Cordis) [20,22]. Microporous polymer-free DES contain a modified surface of pits and holes whose size is of the order of microns. The drug is then coated directly on the rough surface, resulting in the micropores being filled and a nominal layer of drug on top of the surface. The purpose of the micropores is to act as a reservoir for the drug and also to aid adhesion to the stent surface. The rough surface may be created by, for example, a sandblasting technique (Yukon stent, Translumina), or by a microabrasion process (BioFreedom stent, Biosensors Inc.) [23,22]. The VESTAsync stent (MIV Therapeutics) uses a hydroxyapatite surface coating [22]. Hydroxyapatite is an organic porous material that makes up bone mineral and the matrix of teeth and is widely used as a bone substitute. Nanoporous DES are distinguishable from microporous DES by the nature and size of their pores. They exhibit a bulk porous layer (cf. a surface porous layer) and the pores are of the order of nanometres (cf. microns). This layer may be obtained electrochemically (Ceramic-coated TES, Jomed International) or through sputter coating techniques (Setagon stent, Setagon Inc). These stents have the advantage of allowing for a higher drug loading capacity. The Optima stent (CID) contains nanopores too, but the pores are arranged in a regular slotted tubular fashion [23]. Fig. 1(a) displays a nanoporous polymer-free stent whilst 1(b) displays a nanotubular polymer-free stent. Perhaps the most simple polymer-free design is where the drug is coated directly onto the unmodified (relatively) smooth surface of the metal stent. An example of this type of polymer-free DES is the Amazonia Pax (MINVASYS) [22] where a semi-crystalline paclitaxel coating is applied directly to the chromium cobalt stent (see Fig. 1(c)). With no polymer or pores to control the release, it appears that the release rate is determined solely by the solubility and diffusion coefficient of the drug in the release medium and by the thickness of the coating.

Whilst the application of nanoporous drug-eluting coatings to stents is relatively recent, the use of nanoporous surfaces in drug delivery is not new. It is worth briefly mentioning here a few of the other (that is, not stent-based) drug delivery systems that have

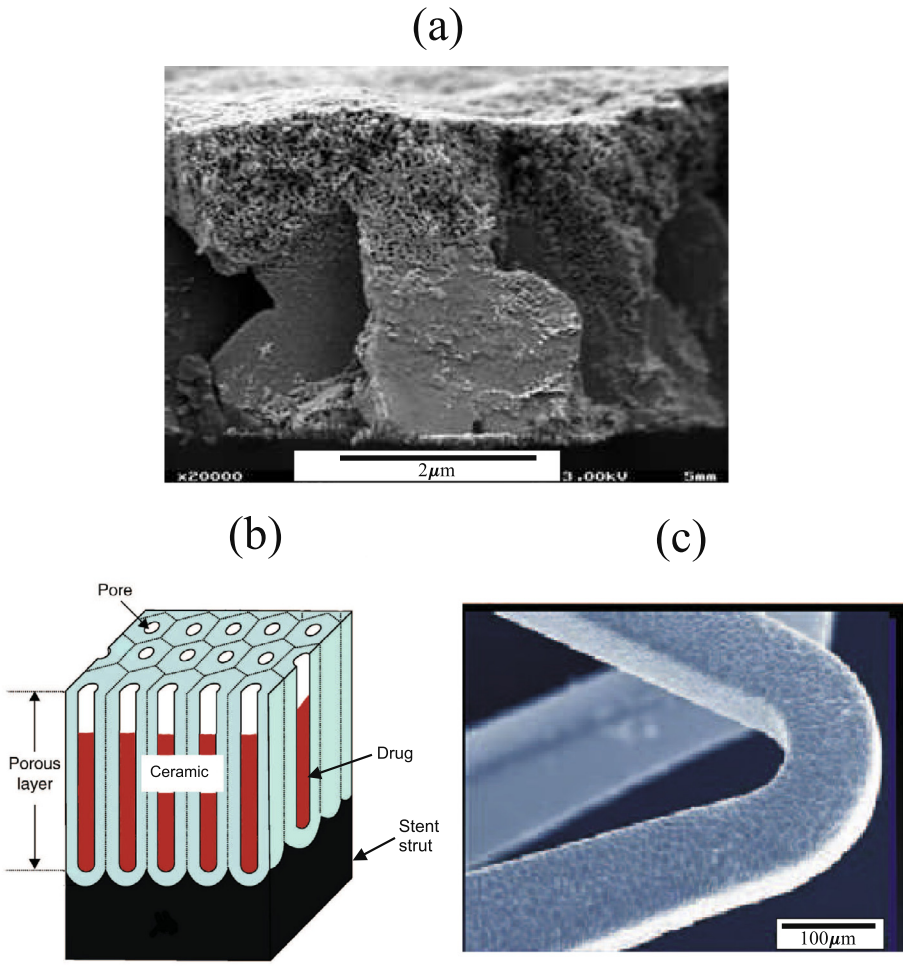

Fig. 1. Some of the polymer-free drug-eluting stent systems modelled in the current study. (a) A scanning electron microscope image of the Setagon stent [20]. A nanoporous drug-infused layer covering a steel strut acts as a reservoir for the prolonged release of drug. The pore diameters here are of the order of 10 nm. (b) A schematic representation of part of a ceramic-coated tacrolimus-eluting stent. The pore diameters here are again of the order of 10 nm. Nanotubular systems of this kind have also been investigated in the context of orthopaedic and dental drug releasing implants. (c) An image of the drug-coated surface of an Amazonia Pax stent [21]. In this polymer-free system, a layer of semi-crystalline paclitaxel of thickness ≈5 μm covers the stent strut surface.

used nanoporous surfaces to release a drug because we believe the model developed in the current study may be applicable to some of these as well. Aw et al. [24] studied the release of drug from a titanium wire into bovine trabecular bone *ex vivo*. The surface of the wire contained nanotubular pits loaded with drug, and the diameter and depth of the nanotubes was of the order of 100 nm and 50 μm, respectively. They experimentally characterised the drug release behaviour, and showed that the drug released into the bone from the nanotubes on a time scale of the order of days. In a similar study, Gulati et al. [25] also considered drug release from nanotubular arrays on titanium wires. They carried out release experiments *in vitro* and observed a two-phase release behaviour, consisting of an initial burst release followed by a zeroth order release over a period of eleven days. Gong et al. [26] studied molecular release from nanoporous alumina capsules, and demonstrated that the release rate could be tuned by varying the diameter of the nanopores.

Although there are a good number of studies that experimentally characterise drug release from nanoporous surfaces, we could only find a few that contain substantive mathematical modelling for drug release from porous metallic or metalloid surfaces. We mention three of these here. Tzur-Balter et al. [27] used a linear diffusion model to describe the release of an anti-cancer drug from nanostructured porous silicon, and found good agreement between their theory and experimental results. In Martin et al. [28], a diffusion model for drug release from silicon nanoporous membranes is verbally described. This model sets a saturation value for the diffusive flux based on the molecular dimensions of the drug and the diameter of the nanopores, and described their experimental release data well. Gultepe et al. [29] took a different approach, opting to describe the release of the drug doxorubicin from nanoporous titanium and aluminium templates using a surface desorption model. In this model, the rate of drug desorption was assumed to take an Arrhenius form and the activation energy was assumed to quadratically depend on the surface coverage of drug.

1.2. Outline

In this paper, rather than focusing on one or more commercially available stents, we provide a generalised model to describe the elution of drug from a range of polymer-free DES. Since the majority of macroporous stents and several microporous stents now actually include a polymer-drug formulation within the pores, we neglect these classes of DES in the analysis that follows. We start by writing down a model for drug release from a nanoporous system. By making some reasonable assumptions, we derive an analytical solution to the model which allows for immediate calculation of the drug release profile. We then proceed to demonstrate how slotted tubular nanoporous DES and smooth surface DES can be shown to be special cases of the generalised model. We provide a model for the two-stage release of the drug from a stent which has a pure drug layer on the surface and a nanoporous drug layer below the surface. Finally, we determine the important parameters characterising the system that govern the drug release, and provide design recommendations so that the release profile may be tailored to achieve the desired outcome. We wish to stress that the models presented here are for drug release in an in vitro environment. Whilst the in vivo release profile will undoubtedly be different (due to a multitude of factors including pulsatile flowing blood, drug binding to proteins and tissue, and wound healing), we believe that it is essential to try to understand the release of drug in a controlled in vitro environment before embarking on the more complex in vivo case. Furthermore, for many cases, in vitro drug release profiles have been shown to be good predictors of in vivo profiles. In addition to this, stent manufactures routinely test the release of drug from their stents in an in vitro environment since it allows them to compare the release profile between different designs [30].

2. Mathematical methods

2.1. The general model for an unstirred release medium

We now formulate a mathematical model for a nanoporous DES system, which includes smooth surface DES and slotted nanotubular DES as special cases. Fig. 2 schematically depicts the nanoporous system, as well as the smooth surface and nanotubular subcases. A two-stage system consisting of a pure drug layer overlaying a drug-infused porous medium will also be considered, and this system is schematically depicted in Fig. 3.

We suppose that the system is one-dimensional, and denote by x the spatial variable as shown in Fig. 2. One-dimensional treatment of drug release from drug-eluting stents has featured heavily in the literature over the past decade (e.g. [9,30–32]). Whilst this type of treatment is a mathematical idealisation of the underlying three-dimensional geometry, it is justified mathematically since the drug release predominantly takes place in the direction normal to the stent surface, owing to the relatively small thickness of the drug layer in comparison to the lateral dimensions. This type of modelling approach has been justified by using a combination of one-dimensional mathematical modelling and experimentation (e.g. [8,31]). We denote by $c_p(x,t)$ and $c_w(x,t)$ the concentration of drug in the liquid-filled pores and in the aqueous medium, respectively, where t is time. The drug may become bound (or "stuck") in a region close to the walls of the pores, and we denote by $c_b(x,t)$ the concentration of immobile drug in this region. The volume fraction of this region is denoted by ϕ_b, and the volume fraction of the pores (the porosity) is denoted by ϕ.

The drug concentration in the pores is assumed to be governed by

$$\phi\frac{\partial c_p}{\partial t} = D_e\frac{\partial^2 c_p}{\partial x^2} - \phi k_a c_p + \phi_b k_d c_b, \qquad s(t) < x < 0, \quad t > 0, \tag{1}$$

where D_e is the effective diffusion coefficient for the drug in the porous medium (see below), and k_a, k_d are the rate constants for drug absorption ("sticking") and desorption ("unsticking"), respectively. The moving boundary $x = s(t)$ locates the interface between the undissolved drug and the aqueous release medium, and will be determined as part of the solution to an initial boundary value problem; see Fig. 2. If L_d is the initial thickness of the drug layer through the porous medium, then $c_p(x,t) = c_0$ for $-L_d < x < s(t)$, $t > 0$, where c_0 is the (assumed) constant concentration of the undissolved drug.

The effective diffusivity D_e in (1) incorporates a number of effects that can arise for diffusion in porous media. If D_w is the free aqueous diffusion coefficient for the drug, then

$$D_e = \frac{\phi_e}{\tau}D_w, \tag{2}$$

where ϕ_e is the effective porosity of the medium and τ is its tortuosity [33]. Both of these parameters are dimensionless and their ratio ϕ_e/τ is one of the key microstructural parameters in the system. The effective porosity ϕ_e refers to the porosity that can contribute to solute transport through the medium, and this can be smaller than the overall porosity ϕ. For example, $\phi_e < \phi$ if the medium contains small pores that the solute cannot access: in this case we say that there is constrictivity. The tortuosity τ takes account of the fact that the particles may have to travel through an increased path length due to the circuitous nature of the pores. Tortuosities usually range in value between two and six, and have an average value of about three [33]. Tortuosity provides another degree of

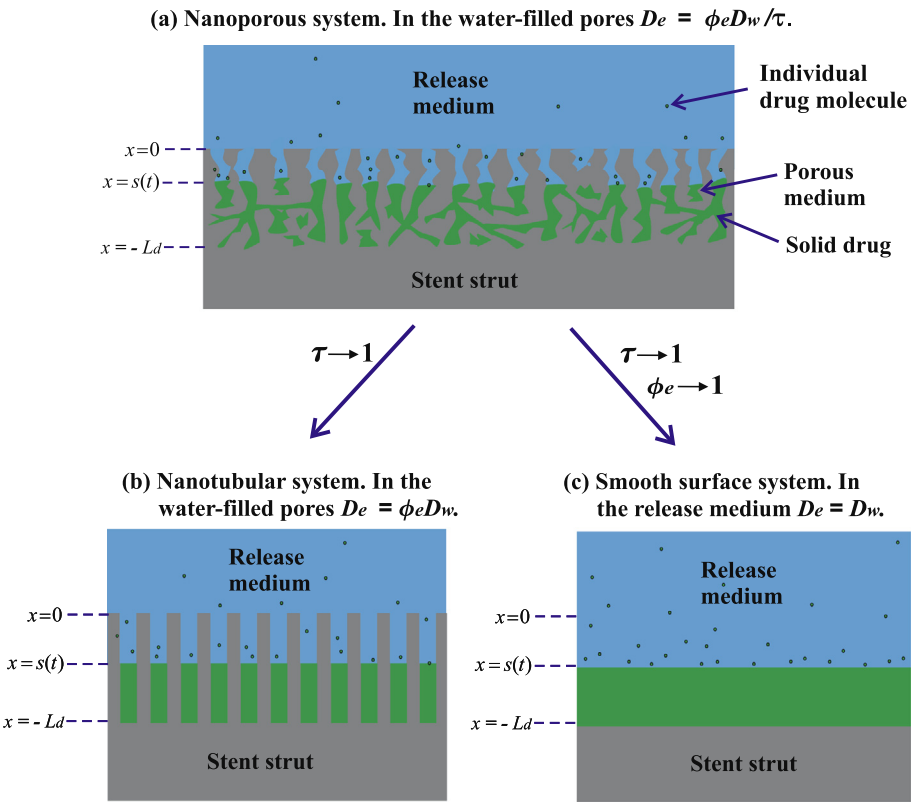

Fig. 2. (a) The stent drug delivery system. A drug-infused porous medium overlays the stent strut. In the liquid-filled pores, the drug has diffusivity $D_e = \phi_e D_w/\tau$, where ϕ_e is the effective porosity of the medium and τ is its tortuosity. In the diagram, $x = 0$ locates the interface between the porous medium and the release medium, and the boundary $x = s(t)$ denotes the position of a moving dissolution front separating the undissolved and dissolved drug. (b) Taking the limiting case of the tortuosity tending to one ($\tau \to 1$) gives the case of a nanotubular system. (c) Taking the limiting case of $\tau, \phi, \ \phi_e \to 1$ and $\phi_b, \ 1/K \to 0$ gives the case of a pure drug layer with no porous medium.

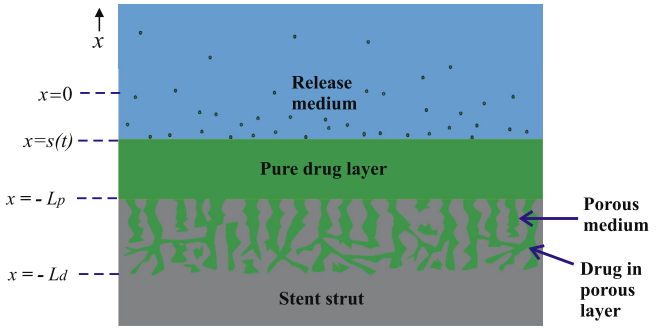

Fig. 3. The system discussed in Section 3.1.4. A pure layer of drug overlays a drug-infused nanoporous medium. This system is capable of exhibiting a two stage release behaviour since the drug release from the pure drug layer is more rapid than that from the porous medium. The system is shown here at a time when the pure drug layer is still dissolving.

freedom to modulate the drug release rate. It is clear that the nanotubular system depicted in Fig. 2(b) will have a smaller tortuosity than a system for which the pores are randomly oriented (see Fig. 2(a)).

The concentration of bound drug in the region close to the pore walls, $c_b(x,t)$, satisfies

$$\phi_b \frac{\partial c_b}{\partial t} = \phi k_a c_p - \phi_b k_d c_b, \qquad s(t) < x < 0, \quad t > 0. \tag{3}$$

Adding (1)–(3) gives the following evolution equation for the total drug in the porous medium

$$\frac{\partial}{\partial t}\left(\phi c_p + \phi_b c_b\right) = D_e \frac{\partial^2 c_p}{\partial x^2}. \tag{4}$$

Assuming that the desorption and absorption rates are fast compared to the diffusion rate, we can replace (3) by the equilibrium expression

$$\phi k_a c_p = \phi_b k_d c_b \quad \text{so that} \quad c_b = \phi c_p/(\phi_b K), \tag{5}$$

where $K = k_d/k_a$ is the equilibrium 'dissociation' constant. In the current study, all of the analytical results presented will be for this case. Numerical solutions based on a front-tracking finite difference scheme have been calculated for the non-equilibrium case, and show excellent agreement with the analytical results for those cases where diffusion is the slowest process. Substituting (5) into (4) gives

$$\frac{\partial c_p}{\partial t} = D_a \frac{\partial^2 c_p}{\partial x^2}, \tag{6}$$

where

$$D_a = \frac{1}{\phi(1+1/K)} D_e = \frac{1}{\tau(1+1/K)} \frac{\phi_e}{\phi} D_w \tag{7}$$

is referred to as the apparent diffusion coefficient, to distinguish it from the effective diffusion coefficient. This single parameter takes account of the effects of porosity, absorption, desorption, tortuosity and constrictivity.

The concentration of drug in the release medium is assumed to be governed by the diffusion equation

$$\frac{\partial c_w}{\partial t} = D_w \frac{\partial^2 c_w}{\partial x^2}, \qquad 0 < x < \infty, \quad t > 0. \tag{8}$$

Eq. (8) does not contain a convection term because we are considering the case of an unstirred fluid here. It is also noteworthy here that the release medium has been taken to be infinite. This is a rea-

sonable assumption given that a typical lengthscale for the release medium is in the centimetre range whilst a typical thickness for the drug-infused porous layer is at least two orders of magnitude smaller.

The case of a well-stirred release medium will also be considered and will be modelled by imposing an infinite sink boundary condition for the drug at $x = 0$; see Section 3.2. Whilst a consensus panel of experts [34] recommend conducting release experiments under infinite sink conditions, it has also been noted by Seidlitz et al. [35] that sink conditions "do not necessarily exist at a particular in vivo site." Consequently, we have chosen in the current study to consider both the unstirred and infinite sink situations. It may be argued that the consideration of both unstirred and infinite sink conditions corresponds to a treatment of the worst- and best-case scenarios, respectively, from the point of view of speed of drug dissolution. In view of this, the consideration of the two cases is a worthwhile exercise given the uncertainty associated with the in vivo situation.

2.1.1. Boundary and initial conditions for an unstirred release medium

We now supplement the governing equations with appropriate boundary and initial conditions. The initial conditions are chosen to be

$$\begin{aligned} &c_w(x,t=0)=0 && \text{for} \quad x>0, \quad s(t=0)=0,\\ &c_p(x,t=0)=c_0, \quad c_b(x,t=0)=\phi c_0/(\phi_b K) && \text{for} \quad -L_d<x<0. \end{aligned} \tag{9}$$

Since c_p has been taken to measure the concentration of drug *in the fluid* fraction of the porous medium, we impose continuity in drug concentration at the interface between the porous medium and the release medium, so that

$$c_p = c_w \quad \text{on} \quad x=0, \qquad t>0. \tag{10}$$

At the interface between the dissolved and undissolved drug, $x = s(t)$, we impose

$$c_p = c_s \quad \text{on} \qquad x=s(t), \quad t>0, \tag{11}$$

where c_s is the solubility of the drug in aqueous medium. The solubility gives the maximum concentration of drug that may be dissolved in the medium.

We also require conditions for the drug flux at $x = 0$ and $x = s(t)$. These conditions are motivated using the assumption that the total amount of drug in the system is conserved. If A is the planar surface area of the porous medium, then the total amount of drug in the system at time t is

$$\begin{aligned} m(t) &= A\left\{\int_{-L_d}^{s(t)}(\phi c_0+\phi_b c_b(x,0))dx+\int_{s(t)}^{0}(\phi c_p+\phi_b c_b)dx+\int_0^\infty c_w dx\right\}\\ &= A\left\{\int_{-L_d}^{s(t)}(1+1/K)\phi c_0 dx+\int_{s(t)}^{0}(\phi c_p+\phi_b c_b)dx+\int_0^\infty c_w dx\right\}. \end{aligned}$$

Imposing $dm(t)/dt = 0$ then leads to

$$\phi(1+1/K)(c_0-c_s)\frac{ds}{dt}+\int_{s(t)}^{0}\frac{\partial}{\partial t}(\phi c_p+\phi_b c_b)dx+\int_0^\infty\frac{\partial c_w}{\partial t}dx=0,$$

which gives

$$\phi(1+1/K)(c_0-c_s)\frac{ds}{dt}+\left(D_e\frac{\partial c_p}{\partial x}\right)_{x=0^-}-\left(D_e\frac{\partial c_p}{\partial x}\right)_{x=s(t)^+}-\left(D_w\frac{\partial c_w}{\partial x}\right)_{x=0^+}=0, \tag{12}$$

where we have imposed $\partial c_w/\partial x \to 0$ as $x \to \infty$. Inspecting this last equation leads to the following choice for the boundary conditions

$$-D_e\frac{\partial c_p}{\partial x}=-D_w\frac{\partial c_w}{\partial x} \quad \text{on} \quad x=0, \quad t>0, \tag{13}$$

Table 1
Values for the parameters appearing in the mathematical model of nanoporous drug release.

Parameter	Range considered	Default value	References
L_d	$10^{-6}-10^{-4}$ m	10^{-4} m	[11,36,7]
D_w	$10^{-11}-10^{-9}$ m^2 s^{-1}	10^{-10} m^2 s^{-1}	[37,38]
c_0/c_s	1.5 – 100	10	
K	0.01 – 10	0.1	
ϕ	$0<\phi<1$	0.6	
ϕ_e	$0<\phi_e\leqslant\phi<1$	0.6	[33]
ϕ_b	$0<\phi_b<\phi_e\leqslant\phi<1$	0.1	
τ	1 – 6	3	[33]

and

$$-D_a\frac{\partial c_p}{\partial x}=\frac{ds}{dt}(c_s-c_0) \quad \text{on} \quad x=s(t), \quad t>0. \tag{14}$$

This last equation gives a so-called Stefan condition to determine the motion of the moving boundary. The final boundary condition is

$$c_w \to 0 \quad \text{as} \quad x\to\infty, \quad t>0. \tag{15}$$

2.2. Parameter values

Given that nanoporous DES are a relatively new technology which have yet to be refined, we consider a range of parameter values (see Table 1) rather than trying to model an existing system. In any case, a complete data set is not readily available for any of the existing systems. We choose our range of values of L_d based on the strut thickness of currently available stents and the thickness of typical DES polymer coatings. The drug diffusion coefficients are representative of the aqueous diffusivities of molecules of similar size to those coated on DES. Since these molecules are known to be poorly soluble we allow for high ratios of c_0/c_s. There would appear to be no data in the literature for the equilibrium 'dissociation' constant and so we consider a range of values for this parameter spanning four orders of magnitude. Finally we choose values of ϕ, ϕ_e and ϕ_b such that $0<\phi_b<\phi_e\leqslant\phi<1$.

3. Results and discussion

3.1. General solution for the unstirred case

For convenience, we gather together here the equations constituting the initial boundary value problem for the unstirred case

$$\begin{aligned} &\frac{\partial c_w}{\partial t}=D_w\frac{\partial^2 c_w}{\partial x^2}, \qquad 0<x<\infty, \quad t>0,\\ &\frac{\partial c_p}{\partial t}=D_a\frac{\partial^2 c_p}{\partial x^2}, \quad c_b=\phi c_p/(\phi_b K), \qquad s(t)<x<0, \quad t>0,\\ &c_p=c_w, \quad -D_e\frac{\partial c_p}{\partial x}=-D_w\frac{\partial c_w}{\partial x} \qquad \text{on} \quad x=0, \quad t>0,\\ &c_p=c_s, \quad -D_a\frac{\partial c_p}{\partial x}=\frac{ds}{dt}(c_s-c_0) \qquad \text{on} \quad x=s(t), \quad t>0,\\ &c_w\to 0 \quad \text{as} \quad x\to+\infty, \qquad t>0, \quad c_w=0 \quad \text{at} \quad t=0, \quad x>0,\\ &c_p=c_0 \text{ at } t=0, \qquad -L_d<x<0, \quad s(t=0)=0. \end{aligned} \tag{16}$$

This problem is self-similar in the Boltzmann variable $x/\sqrt{t}$, and we may write

$$c_w=F(\eta), \quad c_p=G(\eta), \quad \eta=x/\sqrt{t}, \quad s(t)=-\theta\sqrt{t},$$

where θ is a constant, to obtain

$$F''(\eta)+\frac{\eta}{2D_w}F'(\eta)=0,\quad 0<\eta<\infty,\qquad G''(\eta)+\frac{\eta}{2D_a}G'(\eta)=0,\quad -\theta<\eta<0,$$
$$F(0)=G(0),\quad -D_wF'(0)=-D_eG'(0),$$
$$G(-\theta)=c_s,\quad -D_aG'(-\theta)=-\frac{\theta}{2}(c_s-c_0),\quad F(\infty)=0. \tag{17}$$

We note that if the Boltzmann reduction $\eta = x/\sqrt{t}$ is to be valid, then the moving boundary $x = s(t)$ must be expressible as $\eta = \text{const.}$ or $x = \text{const.}\sqrt{t}$, explaining the decision to write $s(t) = -\theta\sqrt{t}$ above. It is clear from (17) that the attempted similarity reduction has in fact led to a consistent two point boundary value problem for a system of ordinary differential equations. Some discussion of the analytical solution of moving boundary problems arising in diffusive systems can be found in Crank [39].

Integrating Eqs. $(17)_1$ for F and G twice gives

$$F(\eta)=\alpha_1\mathrm{erf}\left(\frac{\eta}{2\sqrt{D_w}}\right)+\alpha_2,\quad G(\eta)=\alpha_3\mathrm{erf}\left(\frac{\eta}{2\sqrt{D_a}}\right)+\alpha_4,$$

where α_1, α_2, α_3, α_4 are constants whose values are fixed using the boundary conditions in (17). A straightforward calculation shows that

$$F(\eta)=\frac{c_s\mathrm{erfc}\left(\frac{\eta}{2\sqrt{D_w}}\right)}{1-\frac{\sqrt{D_aD_w}}{D_e}\mathrm{erf}\left(-\frac{\theta}{2\sqrt{D_a}}\right)},\quad 0<\eta<\infty,$$
$$G(\eta)=\frac{c_s\left\{1-\frac{\sqrt{D_aD_w}}{D_e}\mathrm{erf}\left(\frac{\eta}{2\sqrt{D_a}}\right)\right\}}{1-\frac{\sqrt{D_aD_w}}{D_e}\mathrm{erf}\left(-\frac{\theta}{2\sqrt{D_a}}\right)},\quad -\theta<\eta<0, \tag{18}$$

where θ is determined by solving

$$\frac{\theta}{2\sqrt{D_a}}\exp\left(\frac{\theta^2}{4D_a}\right)\left\{1-\frac{\sqrt{D_aD_w}}{D_e}\mathrm{erf}\left(-\frac{\theta}{2\sqrt{D_a}}\right)\right\}=\frac{1}{\sqrt{\pi}}\frac{\sqrt{D_aD_w}}{D_e}\frac{c_s}{c_0-c_s}. \tag{19}$$

We investigated the real solutions of (19) using elementary techniques and with the aid of the mathematical package MAPLE. We found that for positive parameter values and $c_0 > c_s$, two cases arise. For $\sqrt{D_aD_w} < D_e$, there is one positive real root for θ, and of course, this is the required solution. However, for $\sqrt{D_aD_w} > D_e$, there is one positive real root and one negative real root, with the positive choice being the physically relevant one in the current context.

In the original variables, this solution is given by

$$c_w(x,t)=\frac{c_s\mathrm{erfc}\left(\frac{x}{2\sqrt{D_wt}}\right)}{1-\frac{\sqrt{D_aD_w}}{D_e}\mathrm{erf}\left(-\frac{\theta}{2\sqrt{D_a}}\right)},\qquad 0<x<\infty,\quad t>0,$$
$$c_p(x,t)=\frac{c_s\left\{1-\frac{\sqrt{D_aD_w}}{D_e}\mathrm{erf}\left(\frac{x}{2\sqrt{D_at}}\right)\right\}}{1-\frac{\sqrt{D_aD_w}}{D_e}\mathrm{erf}\left(-\frac{\theta}{2\sqrt{D_a}}\right)},\qquad -\theta\sqrt{t}<x<0,\quad t>0. \tag{20}$$

Fig. 4 displays normalised concentration profiles of drug within the pores and in the release medium at four different times within the first day of elution, as calculated from Eqs. (20). Whilst the release medium is taken to be infinite as explained in Section 2.1, for the purposes of this plot we display the release medium normalised drug concentration over a region tenfold greater than that of the thickness of the pores. The profiles are in line with our expectations: to the left of $x = 0$ we observe the moving boundary retreating towards the base of the pores as drug is dissolved and released into the release medium to the right of $x = 0$.

We denote by t_d the time it takes for the moving boundary to reach the bottom of the porous layer, so that $s(t_d) = -L_d$, and

$$t_d = L_d^2/\theta^2. \tag{21}$$

This quantity gives a sensible measure for the drug release lifetime of the device. From (19), it is clear that $s(t)$ has the functional form

$$s(t)=\sqrt{D_at}H\left(\frac{c_s}{c_0},\frac{D_aD_w}{D_e^2}\right)=\sqrt{D_at}H\left(\frac{c_s}{c_0},\frac{\tau}{\phi\phi_e(1+1/K)}\right),$$

for some function H, and then it follows that t_d has the structure

$$t_d=\frac{L_d^2}{D_a}P\left(\frac{c_s}{c_0},\frac{D_aD_w}{D_e^2}\right)=\frac{L_d^2}{D_a}P\left(\frac{c_s}{c_0},\frac{\tau}{\phi\phi_e(1+1/K)}\right).$$

where $P \equiv 1/H^2$. We denote by $M(t)$ the amount of drug that has dissolved in the drug-filled pores by time t. This is simply the volume of the liquid-filled pores multiplied by c_0, so that

$$M(t) = -\phi As(t)c_0 = \theta\phi Ac_0\sqrt{t},$$

and $M(t_d) = M(\infty) = \phi AL_dc_0$. The fraction $M(t)/M(\infty)$ gives the ratio of the drug that was originally in the pores that has dissolved by time t, and is given by

$$\frac{M(t)}{M(\infty)}=\begin{cases}\theta\sqrt{t}/L_d & \text{for}\quad 0\leqslant t\leqslant L_d^2/\theta^2,\\ 1 & \text{for}\quad t>L_d^2/\theta^2.\end{cases} \tag{22}$$

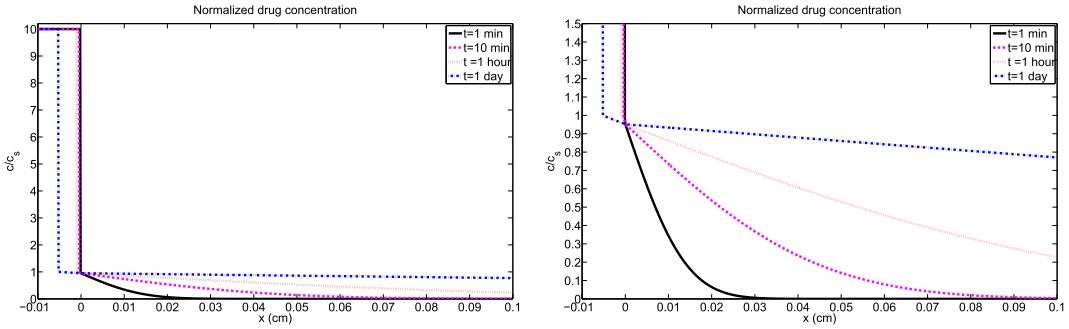

Fig. 4. Normalised concentration profiles of drug in liquid-filled pores, c_p/c_s ($x < 0$), and in the release medium, c_w/c_s ($x > 0$) at four different times. The plot on the right is simply a magnification of the release medium drug concentration profiles that are displayed in the plot on the left. The parameter values used in the generation of this plot are displayed in Table 1.

In the current study, plots of $M_{\%}(=100\times M(t)/M(\infty))$ versus t will be referred to as release profiles. Technically, t_d is the time to dissolution and thus at time t_d some drug will still be contained within the pores (both bound and unbound). Thus $M_{\%}$ is likely to underestimate what we usually mean by release profile: the percentage of drug that has left the device and has entered the release medium. The drug release rate is defined to be the rate of change of $M(t)/M(\infty)$, and is given here by

$$\frac{d}{dt}\left(\frac{M(t)}{M(\infty)}\right)=\begin{cases}\theta/(2\sqrt{t}L_d) & \text{for} \quad 0\leqslant t\leqslant L_d^2/\theta^2,\\ 0 & \text{for} \quad t>L_d^2/\theta^2.\end{cases} \tag{23}$$

We now highlight some notable special cases and extensions of the above solution.

3.1.1. A nanotubular system

The nanotubular system depicted in Fig. 1(b) is modelled by simply letting $\tau\to 1$ in the preceding results, so that $D_e\to\phi_e D_w$ and $D_a\to\frac{1}{(1+1/K)}\frac{\phi_e}{\phi}D_w$.

3.1.2. A smooth surface system

Here we consider the case depicted in Fig. 2(c), in which a layer of pure drug of thickness L_d overlays a stent strut with a smooth surface. The solution for this case can be extracted from the solution displayed in Section 3.1 by letting $\phi,\phi_e\to 1,\ 1/K\to 0$, to obtain ($c_p$ becomes c_w here)

$$s(t)=-\theta\sqrt{t}, c_w(x,t)=c_s\frac{\operatorname{erfc}\left(\frac{x}{2\sqrt{D_w t}}\right)}{\operatorname{erfc}\left(-\frac{\theta}{2\sqrt{D_w}}\right)}, \quad -\theta\sqrt{t}<x<\infty, \quad t>0, \tag{24}$$

where θ is determined by solving

$$\frac{\theta}{2\sqrt{D_w}}\exp\left(\frac{\theta^2}{4D_w}\right)\operatorname{erfc}\left(-\frac{\theta}{2\sqrt{D_w}}\right)=\frac{1}{\sqrt{\pi}}\frac{c_s}{c_0-c_s}. \tag{25}$$

Fig. 5 displays a comparison between the release profiles of nanoporous, nanotubular and smooth surface systems. We observe that a nanotubular system results in quicker release of drug than a nanoporous system due to less tortuous pores. The smooth surface system results in a dramatic increase in the rate of drug release, since there are no pores to hinder the release of drug. By reducing the porosities alone, we demonstrate that the nanoporous system can be tuned to achieve quicker release profiles.

3.1.3. The low solubility limit, $c_s/c_0\ll 1$

We now consider the behaviour of the solution displayed in Section 3.1 in the limit of low drug solubility in the aqueous medium, $c_s/c_0\ll 1$. This case is important because two of the most common drugs that have been used on DES, paclitaxel and sirolimus, are known to be very poorly soluble in water [40]. For $c_s/c_0\ll 1$, it follows from (19) that $\theta/\sqrt{D_a}\ll 1$, and

$$\theta\approx\frac{2}{\sqrt{\pi}}\frac{D_a}{D_e}\frac{c_s}{c_0}\sqrt{D_w},$$

so that

$$s(t)\approx-\frac{2}{\sqrt{\pi}}\frac{1}{\phi(1+1/K)}\frac{c_s}{c_0}\sqrt{D_w t} \qquad \text{for} \quad c_s/c_0\ll 1,$$

making explicit the dependence of the dissolution rate on the porosity, binding properties, and drug solubility. It follows that

$$c_w(x,t)\approx c_s\operatorname{erfc}\left(\frac{x}{2\sqrt{D_w t}}\right) \qquad \text{for} \quad 0<x<\infty, \quad t>0, \tag{26}$$

$$c_p(x,t)\approx c_s \qquad \text{for} \quad -\theta\sqrt{t}<x<0, \quad t_d\approx\frac{\pi}{4}\phi^2(1+1/K)^2\left(\frac{c_0}{c_s}\right)^2\frac{L_d^2}{D_w},$$

for $c_s/c_0\ll 1$. It is noteworthy here that the time it takes for the dissolution front to reach the bottom of the drug layer, t_d, is proportional to the square of the large parameter c_0/c_s, so that the behaviour is strongly dependent on the solubility. This is clearly seen by the large variation in drug release profiles when c_0/c_s is increased from 2 to 20 in Fig. 6. We observe that c_0/c_s has a dramatic influence on the rate of release of the drug. The implication is that if release is to be maintained over a sufficiently long period then drugs that exhibit a low solubility in the release medium are to be preferred. This is supported by clinical data, which shows that DES (almost) exclusively use lipophilic compounds (limited water solubility).

3.1.4. Two stage release

In this section we consider the case of drug release from a system where the release is in two distinct stages. The initial phase is release from a pure drug layer on the surface of the stent, as

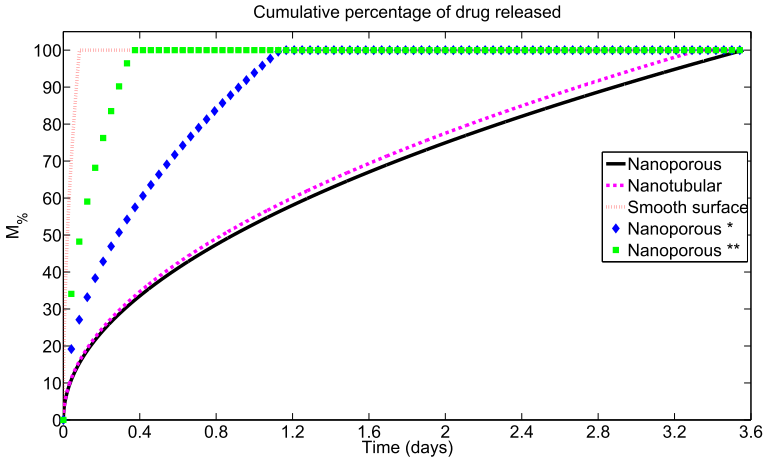

Fig. 5. A comparison between the cumulative percentage of drug released ($M_{\%}$) for a nanoporous, nanotubular and smooth surface system. We observe that a nanotubular system results in quicker release of drug than a nanoporous system due to less tortuous pores. The smooth surface system results in a dramatic increase in the rate of drug release, since there are no pores to hinder the release of drug. Two additional cases have been added to demonstrate one way in which the nanoporous system can be tuned to achieve quicker release profiles. Nanoporous* and Nanoporous** have the reduced porosities $\phi=\phi_e=0.3$ and $\phi=\phi_e=0.1$, respectively. The default parameter values used in the generation of this plot are displayed in Table 1.

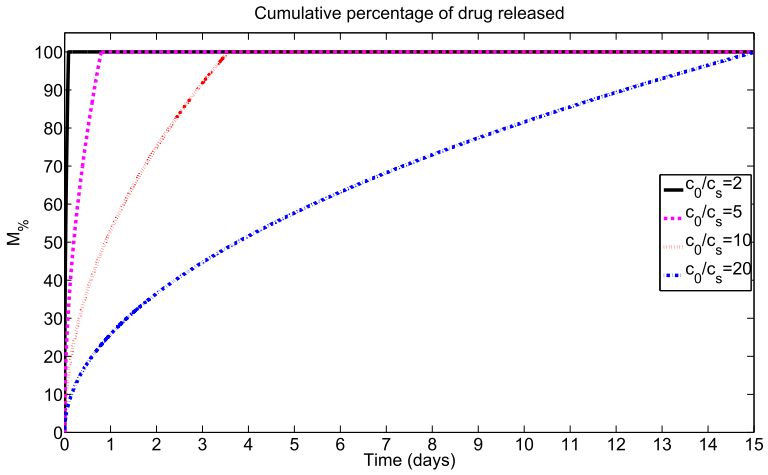

Fig. 6. In this plot we investigate the effect on the cumulative percentage of drug released ($M_{\%}$) with increasing ratio of initial drug concentration to drug solubility, c_0/c_s, for the nanoporous system. We observe that this parameter has a dramatic influence on the rate of release of drug. Increasing this parameter (by either increasing the initial drug concentration or reducing the solubility of the drug in the release medium) can result in a prolonged duration of release. The implication is that if release is to be maintained then drugs that exhibit a low solubility in the release medium are to be preferred. The default parameter values used in the generation of this plot are displayed in Table 1.

described by the equations presented in Section 3.1.2. When all of the surface coated drug has dissolved, drug stored within the nanopores is then released. Here we denote by L_p the initial thickness of the pure drug layer and by L_d the total thickness of the drug layer and the porous medium (see Fig. 3).

This system does not correspond to a special case of the solution (20) because the similarity structure is destroyed by the non-uniform distribution of drug in the release medium when the pure layer has dissolved, and so it must be considered separately. The time for the pure drug layer to dissolve is given by t_p, where $t_p = L_p^2/\theta^2$ and θ is determined by solving (25). For $0 < t < t_p$, the pure drug dissolution phase, the solution is as described in Section 3.1.2. For $t > t_p$, when the drug is released from the nanopores, the governing equations are

$$
\begin{aligned}
&\frac{\partial c_w}{\partial t} = D_w \frac{\partial^2 c_w}{\partial x^2}, \qquad -L_p < x < \infty, \quad t > t_p,\\
&\frac{\partial c_p}{\partial t} = D_a \frac{\partial^2 c_p}{\partial x^2}, \quad c_b = \phi c_p/(\phi_b K), \qquad s(t) < x < -L_p, \quad t > t_p,\\
&c_p = c_w, \quad -D_e \frac{\partial c_p}{\partial x} = -D_w \frac{\partial c_w}{\partial x} \qquad \text{on} \quad x = -L_p, \quad t > t_p,\\
&c_p = c_s, \quad -D_a \frac{\partial c_p}{\partial x} = \frac{ds}{dt}(c_s - c_0) \qquad \text{on} \quad x = s(t), \quad t > t_p,\\
&c_w \to 0 \qquad \text{as} \quad x \to +\infty, \quad t > t_p, \quad c_w = c_s \frac{\operatorname{erfc}\left(\frac{x}{2\sqrt{D_w t_p}}\right)}{\operatorname{erfc}\left(-\frac{\theta}{2\sqrt{D_w}}\right)}\\
&\text{at} \quad t = t_p, \quad x > -L_p,\\
&c_p = c_0 \qquad \text{at} \quad t = t_p, \quad -L_d < x < -L_p, \quad s(t = t_p) = -L_p.
\end{aligned}
\tag{27}
$$

This problem does not admit a similarity reduction, and is not solved here analytically. However, analytical progress can be made by considering the asymptotic limit $D_a/D_w \to 0$, with $1/K$ and all of the other dimensionless parameters being held $O(1)$; see Holmes [41] for a discussion of relevant asymptotic methods. This corresponds to the case of slow drug diffusion in the porous medium compared to that in the release medium. We omit almost all of the asymptotic details here, confining ourselves instead to quoting the result that is of most interest from the point of view of applications. Writing $\varepsilon = D_a/D_w$ and taking the limit $\varepsilon \to 0$, it is found that the total amount of drug released by time t is given by

$$
M(t) \sim \begin{cases} \theta\sqrt{t}Ac_0 & \text{for} \quad 0 \leqslant t \leqslant t_p, \quad t = O(L_d^2/D_w),\\ (L_p + \rho\phi\sqrt{\varepsilon D_w(t - t_p)})Ac_0 & \text{for} \quad t_p < t < t_d, \quad t = t_p + O(L_d^2/\{\varepsilon D_w\}),\\ (L_p + \phi(L_d - L_p))Ac_0 & \text{for} \quad t \geqslant t_d, \end{cases}
\tag{28}
$$

where t_d is the dissolution time, θ is found from (25), and ρ satisfies

$$
\frac{\rho}{2}\exp\left(\frac{\rho^2}{4}\right)\operatorname{erf}\left(-\frac{\rho}{2}\right) = -\frac{1}{\sqrt{\pi}}\frac{c_s}{c_0 - c_s}.
$$

As would be expected, Eq. (28) predicts a two stage release rate with relatively rapid release for $t < t_p$ when the pure drug is dissolving, and a slow release for $t_p < t < t_d$ when the drug is releasing from the porous medium. At leading order, the solution for $t > t_p$ has the same form as the solution for release into a well-stirred medium, and this case is considered in the next section.

The problem (27) has also been solved numerically using a front-tracking method, and a description of the numerical method used can be found in the Supplementary Material. This method is based on a front-tracking scheme described in Crank [39]. In Fig. 7, we display the cumulative fraction of drug released from a two-stage release system for various values of D_a corresponding to varying the value of K. We observe two distinct phases of release. In the first phase a large amount of surface layer drug is dissolved rapidly, whilst in the second phase release of drug from the nanopores proceeds at a considerably slower rate. The effect of reducing the parameter K is to prolong the duration of the second phase of release.

3.2. General solution for the well-stirred case

For a well-stirred release medium, we assume a very low concentration for the drug in the medium, and replace Eq. (10) by

$$
c_p = 0 \qquad \text{on} \quad x = 0, \quad t > 0,
\tag{29}
$$

so that $x = 0$ acts as a perfect sink for dissolved drug in the liquid-filled pores. The boundary and initial conditions (11) and (9) remain unchanged. It should be emphasised here that the well-stirred case is of particular importance because many release experiments are conducted under well-stirred conditions. Perfect sink boundary

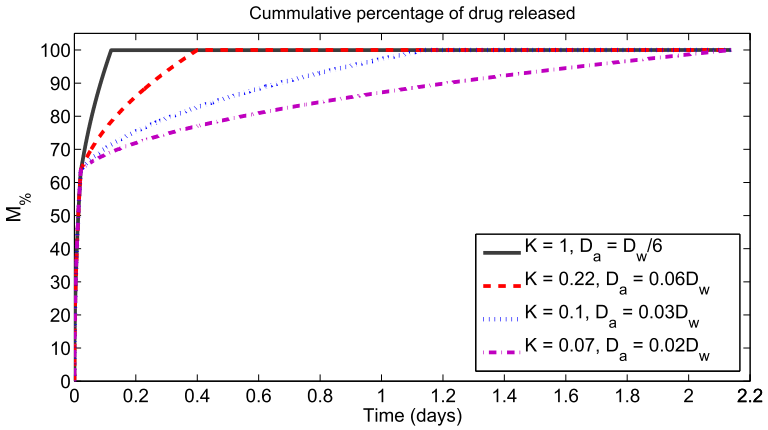

Fig. 7. Plot of the cumulative fraction of drug released from a two-stage release system for various D_a/D_w corresponding to varying K. Here we plot the numerical solution for the default parameter values in Table 1 except that $L_p = 5 \times 10^{-5}$ m and $L_d = 10^{-4}$ m.

conditions can also be appropriate if the release medium is regularly replaced in the experiments. We need only solve for $c_p(x,t)$ and $s(t)$. The solution has the similarity structure $c_p = c_p(x/\sqrt{t})$, $s(t) = -\theta\sqrt{t}$, and we find that

$$c_p(x,t) = c_s \frac{\operatorname{erf}\left(\frac{x}{2\sqrt{D_a t}}\right)}{\operatorname{erf}\left(-\frac{\theta}{2\sqrt{D_a}}\right)}, \qquad -\theta\sqrt{t} < x < 0, \quad t > 0, \tag{30}$$

where θ is determined from

$$\frac{\theta}{2\sqrt{D_a}} \exp\left(\frac{\theta^2}{4D_a}\right) \operatorname{erf}\left(-\frac{\theta}{2\sqrt{D_a}}\right) = -\frac{1}{\sqrt{\pi}} \frac{c_s}{c_0 - c_s}. \tag{31}$$

For the case of poorly soluble drugs, $c_s/c_0 \ll 1$, (31) gives that $\theta \approx \sqrt{2D_a(c_s/c_0)}$, so that $s(t) \approx -\sqrt{2D_a(c_s/c_0)t}$ and

$$t_d = \frac{L_d^2}{\theta^2} \approx \frac{1}{2} \frac{\phi}{\phi_e} \tau (1 + 1/K) \frac{c_0}{c_s} \frac{L_d^2}{D_w} \qquad \text{for} \quad c_s/c_0 \ll 1. \tag{32}$$

It is instructive to compare this result with the corresponding expression in (26) for the unstirred case. Note that t_d in (26) depends on the square of the large parameter c_0/c_s, whilst (32) depends only on its first power. Hence, for poorly soluble drugs, dissolution is an order of magnitude faster in a well-stirred medium than for an unstirred medium. Of course, faster drug dissolution in the well-stirred medium conforms to our intuitive expectations. In Fig. 8 we display a comparison between the release profiles of drug released from a nanoporous system into unstirred and well-stirred release media. We observe that drug release is significantly sped up in the well-stirred release medium, as one would expect. Also on display are the approximate solutions for poorly soluble drugs, and these show good agreement with the full solution for both the unstirred and well-stirred cases when $c_s/c_0 = 0.1$.

3.2.1. A pure drug layer in a well-stirred release medium

The solution (30), (31) cannot be used to describe the dissolution of a pure drug layer in a well-stirred release medium since the boundary condition $c_p = 0$ on $x = 0$ is not appropriate for this case – there is now no porous medium to maintain the validity of the perfect sink boundary condition at $x = 0$. Drug dissolution in a well-stirred release medium has been the subject of numerous previous studies, and was recently reviewed by Siepmann & Siepmann [42]. We now use these well-established ideas to model this case. The system is as depicted in Fig. 2(c). The moving boundary $x = s(t)$, initially located at $x = 0$, separates the release medium from the pure drug layer, and the initial thickness of the drug layer

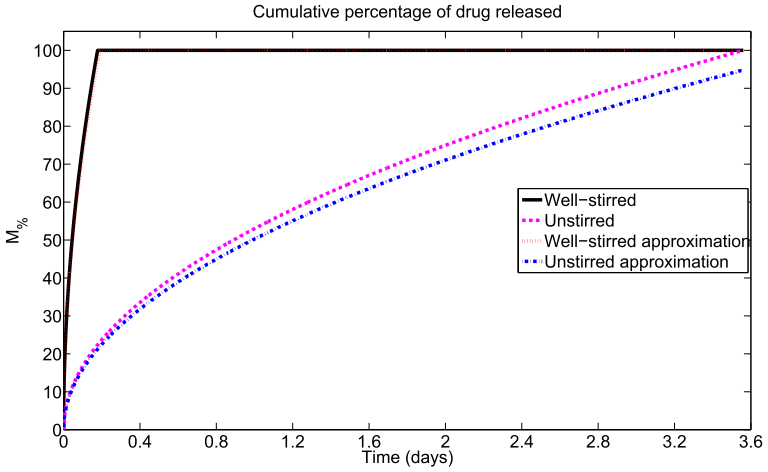

Fig. 8. A comparison between the cumulative percentage of drug released ($M_\%$) from the nanoporous system in unstirred and well-stirred release media. Also on display are the approximate solutions for the case of poorly soluble drugs. In each case we have $c_s/c_0 = 0.1 < 1$. We observe that drug release is significantly sped up in the well-stirred release medium, as one would expect. Furthermore, the respective approximate solutions for poorly soluble drugs are providing good agreement with the full solutions, even for $c_s/c_0 = 0.1$. The agreement improves as c_s/c_0 is reduced further. The default parameter values used in the generation of this plot are displayed in Table 1.

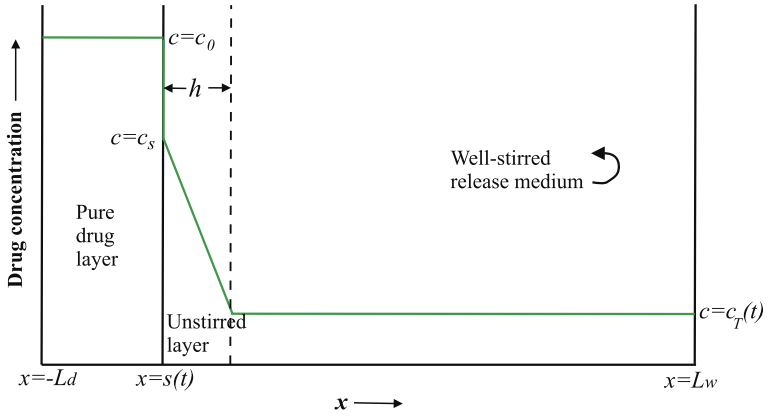

Fig. 9. The special case of a pure drug layer in a well-stirred release medium. This case cannot be described by the solution (30), (31) and must be considered separately. A narrow boundary layer of poorly stirred fluid forms near the surface of the solid drug, and it is assumed that the flux of drug from the dissolving surface is proportional to the difference between the drug concentration at the surface and the drug concentration in the well-stirred release medium.

is L_d. For this case, we shall take the release medium to be finite in extent, and to initially occupy $0 < x < L_w$. When the medium is well-stirred, a boundary layer of poorly stirred fluid forms close to the surface of the dissolving drug layer. This layer is taken to be of thickness h, with the size of h depending on the degree of agitation in the fluid bulk. This is admittedly a somewhat crude characterisation of the behaviour, but it is commonly used, and does lead to a useable theory that gives satisfactory agreement with experimental results [42]. In the current analysis, we take $h \ll L_d \ll L_w$, and denote by $c_T(t)$ the uniform drug concentration in the well-stirred medium at time t. In Fig. 9, we schematically depict the various regions and drug concentrations arising.

The key assumption of the Noyes–Whitney and the Nernst–Brunner dissolution models [43,44] is that the flux of drug from the surface of the dissolving drug layer is proportional to the difference between the concentration of drug in the release medium and the concentration of drug at the surface. Denoting by $j|_{x=s(t)}$, the flux of drug from $x = s(t)$, we write

$$j|_{x=s(t)} = -D_w \frac{(c_T(t) - c_s)}{h}, \tag{33}$$

where c_s is the drug concentration on $x = s(t)$. Eq. (33) is a statement of Fick's first law, with the right hand side of (33) playing the role of $-D_w \partial c/\partial x$ in the more familiar statement of the law. In view of (14), the appropriate equation for the speed of the front is now

$$-D_w \frac{(c_T(t) - c_s)}{h} = \frac{ds}{dt}(c_s - c_0) \qquad \text{on} \quad x = s(t), \quad t > 0. \tag{34}$$

Equating the amount of drug that has dissolved with the amount in the release medium, and using the fact that $h \ll L_d \ll L_w$, we have

$$-s(t)c_0 \approx L_w c_T(t). \tag{35}$$

Combining (34) and (35) leads to

$$\frac{ds(t)}{dt} + \frac{D_w}{hL_w}\frac{c_0}{c_0 - c_s}s(t) \approx -\frac{D_w}{h}\frac{c_s}{c_0 - c_s}, \qquad t > 0,$$

which is solved subject to $s(0) = 0$ to give

$$s(t) \approx -\frac{c_s}{c_0}L_w(1 - \exp(-t/t')),$$

where $t' = hL_wD_w(1 - c_s/c_0)/D_w$ determines the time scale for dissolution. It follows that

$$c_T(t) \approx c_s(1 - \exp(-t/t')).$$

For $t \ll t'$, we have $s(t) \approx -c_sL_wt/(c_0t')$, which clearly distinguishes this case from the $t^{1/2}$ behaviour of the unstirred case.

The time for the drug to dissolve, t_d, is determined from $s(t_d) = -L_d$, which gives

$$t_d \approx -t' \ln\left(1 - \frac{L_dc_0}{L_wc_s}\right),$$

and this quantity is clearly only defined for $L_dc_0 < L_wc_s$. This is as expected since for $L_dc_0 > L_wc_s$ there is sufficient drug to completely saturate the release medium, and the drug cannot then fully dissolve. For $L_dc_0 < L_wc_s$, the release profile is given by

$$\frac{M(t)}{M(\infty)} \approx \begin{cases} \frac{L_wc_s}{L_dc_0}(1 - \exp(-t/t')) & \text{for} \quad 0 \leqslant t \leqslant t_d, \\ 1 & \text{for} \quad t > t_d. \end{cases}$$

3.2.2. Sensitivity analysis of the design parameters

The models we have presented include several parameters which may in principle be altered during the manufacturing of the device. It is therefore of interest to consider the sensitivity of the release profiles to changes in these parameters. Nanoporous systems appear to have the best potential for controlling the drug release since they exhibit the highest number of tunable parameters: porosity, absorption, desorption, tortuosity, constrictivity, thickness of the porous layer, drug diffusivity in the release medium and the ratio of drug solubility to initial drug concentration. Nanotubular systems have tortuosity set to 1 and therefore provide faster drug release. Smooth surface systems result in significantly quicker drug release with the rate of release being controlled purely by the thickness of the drug layer, the ratio of drug solubility to initial drug concentration and the diffusivity of the drug in the release medium. In all of these systems, the thickness of the drug layer L_d is an important parameter since from (21) it is clear that the release time varies as the square of L_d. Thus, in all cases, increasing the value of L_d will result in an increase in the duration of the drug release. Taking the example of the nanoporous one-layer system, if we reduce L_d from 10^{-4} m to 5×10^{-5} m and then 10^{-5} m (using the default parameter values in Table 1), the release time decreases significantly from 3.6 days to 21.4 h to 51.5 min, respectively. Of course, there will undoubtedly be constraints on the value that L_d can take, both from the manufacturing side and also from the physiological viewpoint.

From Eq. (7) we observe that the single parameter D_a takes account of the effects of porosity, absorption, desorption, tortuosity and constrictivity and thus it is of key importance in determining the speed of drug release. Depending on the values of $\phi_e/\tau, K$, and ϕ, the parameter D_a can vary by several orders of magnitude and as a consequence the release time can be significantly delayed. In Table 2 we present calculated release times when these para-

Table 2
Parameter values used in the sensitivity analysis.

Parameter varied	Value of parameter	Value of D_a ($m^2\ s^{-1}$)	Release time, t_d (days)
K	10	3.03×10^{-11}	0.0552
K	1	1.67×10^{-11}	0.165
K	0.1	3.03×10^{-12}	3.56
K	0.01	3.30×10^{-13}	274
ϕ_e/τ	0.6	9.09×10^{-12}	3.33
ϕ_e/τ	0.25	3.79×10^{-12}	3.49
ϕ_e/τ	0.05	7.58×10^{-13}	4.54
ϕ_e/τ	0.01	1.52×10^{-13}	8.96
ϕ	0.9	2.02×10^{-12}	7.75
ϕ	0.8	2.27×10^{-12}	6.18
ϕ	0.7	2.60×10^{-12}	4.78

meters are varied. The parameter K not only has the largest impact on the value of D_a (spanning two orders of magnitude for the values considered), but also has the greatest influence on the release times which increase from 79 min to 274 days when K is decreased from 10 to 0.01. The microstructural parameter ϕ_e/τ has a maximum value of 1, corresponding to the case where the porous region is completely void: in this case, $D_e = D_w = D_a$ ($1/K \to 0$ since there are no pore walls for the drug to stick to). Since this case corresponds to the smooth surface system, we focus on intermediate values of ϕ_e/τ. We observe that this parameter has less of an effect on release times, with the release time increasing by less than 4 h when ϕ_e/τ is reduced by more than half from 0.6 to 0.25. However, as we reduce this parameter further we can prolong the release time: when ϕ_e/τ is reduced to 0.01, the release time is extended to almost 9 days. However, this would correspond to an extremely low effective porosity or extremely tortuous pores. The effect of increasing ϕ (whilst keeping $\phi_e < \phi$ fixed) is to increase the release time since we are effectively increasing the initial mass of drug in the porous layer and so it takes longer to dissolve. In reality, it is likely that the drug coating process will result in a thin layer of drug on the surface of the stent in addition to the drug that is contained within the porous region. If this layer is sufficiently thin then it will have little effect on the release time since the surface layer will be dissolved rapidly. But if the layer is of a non-negligible thickness then two distinct phases of release are observed. The first is a fast phase corresponding to pure drug dissolving on the surface and the second is a slow phase corresponding to drug contained within the nanopores being eluted. By varying the surface layer thickness we can therefore add another degree of tunability. For example, if a large burst of drug is desired initially followed by a slow zero-order release then this can be achieved by tweaking the value of L_p. Thus by varying the parameter values of the system, a stent may in principle be designed to deliver a given amount of drug rapidly, over a defined time period, and then the remainder of the drug slowly, over a longer defined period of time. In Fig. 10, the cumulative fraction of drug released from a two-stage release system is plotted for various values of L_p.

When we analyse the case of nanoporous (or nanotubular) drug release into a well-stirred release medium, we see that the drug release depends purely on the value of D_a and the ratio c_s/c_0. Thus, by varying these parameters as above we can also tailor the release profile for the well-stirred case. As described in Section 3.2, drug dissolution is significantly faster in a well-stirred release medium. This is evidenced in Fig. 8 which compares the release profiles from the nanoporous system in unstirred and well-stirred release media.

4. Conclusions

In this paper we have presented the first model of drug elution from polymer-free drug-eluting stents. Our generalised model is capable of predicting the drug release from a number of systems including nanoporous, nanotubular and smooth surface systems. We have identified the key parameters of the system which may be tuned at the manufacturing stage to achieve the desired drug release profile. In particular, we observed that the duration of release is particularly sensitive to the thickness of the drug layer, the ratio of drug absorption to desorption and ratio of drug solubility to initial drug concentration. Whilst the first two of these may be manipulated during the manufacture of the stent material, the latter will depend on the properties of the particular drug considered (for example whether it is in an amorphous or crystalline phase). Other parameters such as the porosity and tortuosity can be utilised to fine tune a particular release profile. We have also demonstrated that a two-layer system (comprising a pure drug layer on the surface above a porous drug layer) can provide additional flexibility in tuning the release profile. Two distinct phases of release can be obtained, with the duration of each phase and the amount of drug delivered during each phase able to be varied by adjusting the model parameters accordingly.

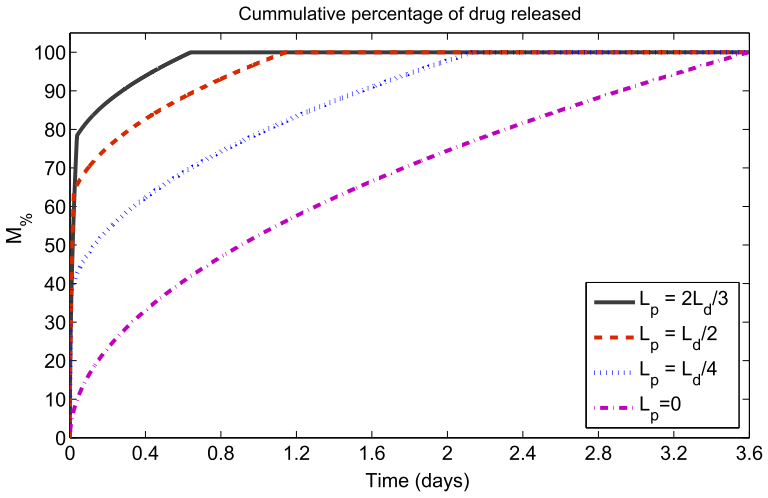

Fig. 10. Plot of the cumulative fraction of drug released from a two-stage release system for various L_p/L_d. Here we plot the numerical solution for the default parameter values in Table 1.

One of the main advantages of the models presented in this work is the ability to achieve analytical solutions. These solutions not only allow for release profiles to be rapidly calculated, but they also clearly show the dependence of the various parameters of the system on the release profiles. This is of great benefit when considering the required design parameters to achieve a particular release profile. We would like to emphasise that the models presented in this paper are for drug release in an in vitro environment since we believe that it is essential to understand the drug release dynamics in a controlled environment before embarking on the in vivo environment. We acknowledge that whilst our work may suggest that a system designed with certain parameter values will give rise to a particular in vitro release profile, the in vivo release profile may be quite different. We have considered in vitro release into both unstirred and well-stirred release media, corresponding to a treatment of the worst- and best-case scenarios, respectively, from the point of view of speed of drug dissolution. We acknowledge that since a stent upon implantation is exposed to tissue at its outer surface and to blood flow at its inner surface, in reality (in vivo) a combination of these two extreme approaches would likely be more appropriate. Furthermore, there may be biological and mechanical constraints on the design of the device which are not considered here.

Acknowledgements

The authors would like to acknowledge funding provided by The Royal Society (grant Reference: IE131240) and EPSRC (Grant No. EP/J007242/1). We would also like to thank Doctor Simon Kennedy (The Institute of Cardiovascular and Medical Sciences, University of Glasgow) and Professor Keith Oldroyd (Consultant Interventional Cardiologist, Golden Jubilee National Hospital, Glasgow) for their helpful suggestions and advice. Dr. Vo and Dr. Meere gratefully acknowledge the support of the Mathematics Applications Consortium for Science and Industry (www.macsi.ul.ie) funded by the Science Foundation Ireland (SFI) Investigator Award 12/IA/1683. Dr. Vo thanks the New Foundations Award 2013 from Irish Research Council. Dr. Meere thanks NUI Galway for the award of a travel grant.

Appendix A. Figures with essential colour discrimination

Certain figures in this article, particularly Figs. 1–10, are difficult to interpret in black and white. The full colour images can be found in the on-line version, at http://dx.doi.org/10.1016/j.actbio.2015.02.006.

Appendix B. Supplementary data

Supplementary data associated with this article can be found, in the online version, at http://dx.doi.org/10.1016/j.actbio.2015.02.006.

References

[1] Stefanini GG, Holmes DR. Drug-eluting coronary artery stents. N Engl J Med 2013;368:254–65.
[2] Khan W, Farah S, Domb AJ. Drug eluting stents: developments and current status. J Control Release 2012;161:703–12.
[3] Nebeker JR, Virmani R, Bennett CL, Hoffman JM, Samore MH, Alvarez J, et al. Hypersensitivity cases associated with drug-eluting coronary stents: a review of available cases from the research on adverse drug events and reports (radar) project. J Am Coll Cardiol 2006;47(1):175–81.
[4] van der Giessen WJ, Lincoff AM, Schwartz RS, van Beusekom HMM, Serruys PW, Holmes DR, et al. Marked inflammatory sequelae to implantation of biodegradable and nonbiodegradable polymers in porcine coronary arteries. Circulation 1996;94(7):1690–7.
[5] Joner M, Finn A, Farb A, Mont E, Kolodgie F, Ladich E, et al. Pathology of drug-eluting stents in humans: delayed healing and late thrombotic risk. J Am Coll Cardiol 2006;48(1):193–202.
[6] Kotani J, Awata M, Nanto S, Uematsu M, Oshima F, Minamiguchi H, et al. Incomplete neointimal coverage of sirolimus-eluting stents. angioscopic findings. J Am Coll Cardiol 2006;47(10):2108–11.
[7] McGinty S, McKee S, Wadsworth RM, McCormick C. Modelling drug-eluting stents. Math Med Biol 2011;28:1–29.
[8] McGinty S, McKee S, Wadsworth RM, McCormick C. Modeling arterial wall drug concentrations following the insertion of a drug-eluting stent. SIAM J Appl Math 2014;73(6):2004–28.
[9] Pontrelli G, de Monte F. Mass diffusion through two-layer porous media: an application to the drug-eluting stent. Int J Heat Mass Trans 2007;50:3658–69.
[10] Zunino P. Multidimensional pharmacokinetic models applied to the design of drug-eluting stents. Cardiov Eng Int J 2004;4(2):181–91.
[11] Bozsak F, Chomaz J, Barakat AI. Modeling transport of drugs eluted from stents: physical phenomena driving drug distribution in the arterial wall. Biomech Model Mechanobiol 2014;13(2):327–47.
[12] Siepmann J, Siepmann F. Mathematical modelling of drug delivery. Int J Pharmaceut. 2008;364:328–43.
[13] Fredenberg S, Reslow MWM, Axelsson A. The mechanisms of drug release in poly(lactic-co-glycolic acid)-based drug delivery systems – a review. Int J Pharmaceut 2011;415:34–52.
[14] Prabhu S, Hossainy S. Modeling of degradation and drug release from a biodegradable stent coating. J Biomed Mater Res A 2007;80A(3):732–41.
[15] Siepmann J, Gopferich A. Mathematical modeling of bioerodible, polymeric drug delivery systems. Adv Drug Deliv Rev 2001;48(2–3):229–47.
[16] Rothstein SN, Federspiel WJ, Little SR. A unified mathematical model for the prediction of controlled release from surface and bulk eroding polymer matrices. Biomaterials 2009;30(8):1657–64.
[17] Soares JS, Zunino P. A mixture model for water uptake, degradation, erosion and drug release from polydisperse polymeric networks. Biomaterials 2010;31(11):3032–42.
[18] Rossi F, Casalini T, Masi ERM, Perale G. Bioresorbable polymer coated drug eluting stent: a model study. Mol Pharm 2012;9(7):1898–910.
[19] Huang Y, Ng H, Ng X, Subbu V. Drug-eluting biostable and erodible stents. J Control Release 2014. http://dx.doi.org/10.1016/j.jconrel.2014.05.011.
[20] Tsujino I, Ako J, Honda Y, Fitzgerald PJ. Drug delivery via nano-, micro and macroporous conronary stent surfaces. Expert Opin Drug Deliv 2007;4(3):287–95.
[21] Minivasys, http://heartbeat.co.in/wp-content/uploads/amazonia-pax-2010.pdf, 2010
[22] Abizaid A, Ribamar-Costa J. New drug-eluting stents: an overview on biodegradable and polymer-free next-generation stent systems. Circ Cardiovasc Interv 2010;3:384–93.
[23] Ma X, Wu T, Robich MP. Drug-eluting stent coatings. Interv Cardiol 2012;4(1):73–83.
[24] Aw M, Khalid K, Gulati K, Atkins G, Pivonka P, Findlay D, Losic D. Characterization of drug-release kinetics in trabecular bone from titania nanotube implants. Int J Nanomed 2012;7:4883–92.
[25] Gulati K, Aw M, Losic D. Drug-eluting Ti wires with titania nanotube arrays for bone fixation and reduced bone infection. Nanoscale Res Lett 2011;571(6). http://dx.doi.org/10.1186/1556-276X-6-571.
[26] Gong D, Yadavalli V, Paulose M, Pishko M, Grimes C. Controlled molecular release using nanoporous alumina capsules. Biomed Microdevices 2003;5(1):75–80.
[27] Tzur-Balter A, Young J, Bonanno-Young L, Segal E. Mathematical modeling of drug release from nanostructured porous Si: combining carrier erosion and hindered drug diffusion for predicting release kinetics. Acta Biomater 2013;9:8346–53.
[28] Martin F, Walczak R, Boiarski A, Cohen M, West T, Cosentino C, Ferrari M. Tailoring width of microfabricated nanochannels to solute size can be used to control diffusion kinetics. J Control Release 2005;102:123–33.
[29] Gultepe E, Nagesha D, Sridhar S, Amiji M. Nanoporous inorganic membranes or coatings for sustained drug delivery in implantable devices. Adv Drug Deliv Rev 2010;62:305–15.
[30] McGinty S, McKee S, McCormick C, Wheel M. Release mechanism and parameter estimation in drug-eluting stent systems: analytical solutions of drug release and tissue transport. Math Med Biol 2014. http://dx.doi.org/10.1093/imammb/dqt025.
[31] Zhao H, Jayasinghe D, Hossainy S, Schwartz L. A theoretical model to characterize the drug release behavior of drug-eluting stents with durable polymer matrix coating. J Biomed Mater Res A 2012;100A(1):120–4.
[32] Hossainy S, Prabhu S. A mathematical model for predicting drug release from a biodurable drug-eluting stent coating. J Biomed Mater Res A 2008;87A:487–93.
[33] Cussler E. Diffusion: mass transfer in fluid systems. third ed. New York: Cambridge University Press; 2009.
[34] Schwartz RS, Edelman E, Virmani R, Carter A, Granada JF, Kaluza GL, et al. Drug-eluting stents in preclinical studies updated consensus recommendations for preclinical evaluation. Circ Cardiovasc Interv 2008;1(7):143–53.
[35] Seidlitz A, Nagel S, Semmling B, Sternberg K, Kroemer HK, Weitschies W. In vitro dissolution testing of drug-eluting stents. Curr Pharm Biotechnol 2013;14:67–75.

[36] Capodanno D, Dipasqua F, Tamburino C. Novel drug-eluting stents in the treatment of de novo coronary lesions. Vasc Health Risk Manage 2011;7:103–18.
[37] Tzafriri AR, Groothuis A, Price GS, Edelman ER. Stent elution rate determines drug deposition and receptor-mediated effects. J Control Release 2012;161:918–26.
[38] Zhu X, Pack DW, Braatz RD. Modelling intravascular delivery from drug-eluting stents with biodurable coating: investigation of anisotropic vascular drug diffusivity and arterial drug distribution. Comput Methods Biomech Biomed Eng 2012;17(3):1–12.
[39] Crank J. Free and moving boundary problems. third ed. New York: Oxford University Press Inc.; 1984.
[40] Simamora P, Alvarez J, Yalkowsky S. Solubilization of rapamycin. Int J Pharm 2001;213:25–9.
[41] Holmes M. Introduction to perturbation methods. second ed. New York: Springer; 2012.
[42] Siepmann J, Siepmann F. Mathematical modeling of dissolution. Int J Pharm 2013;453:12–24.
[43] Noyes A, Whitney W. The rate of solution of solid substances in their own solutions. J Am Chem Soc 1897;19:930–4.
[44] Brunner E. Reaktionsgeschwindigkeit in heterogenen systemen. Z Phys Chem 1904;47:56–102.